JOURNAL OF SPACECRAFT AND ROCKETS
Vol. 42, No. 5, September–October 2005

Artificial Gravity and Abort Scenarios via Tethers for Human Missions to Mars

Michael D. Jokic*
University of Queensland, Brisbane, Queensland 4072, Australia
and
James M. Longuski†
Purdue University, West Lafayette, Indiana 47907-2023

Minimum-mass tether designs are developed for a spinning human transport that not only provides artificial gravity, but also the potential for free-return aborts. The investigation reveals that severing the tether can provide a propellant-free boost to return astronauts to Earth in the event of an aborted landing on Mars. Earth–Mars–Earth, Earth–Mars–Venus–Earth, and Earth–Venus–Mars–Earth trajectories requiring little, or no, velocity change after departure from Earth, are examined. The investigation covers trajectories with launch opportunities between 2014 and 2030, launch hyperbolic excess speeds of up to 4.5 km/s and total flight times of less than 1000 days. We identify propellant-free abort scenarios in every Earth–Mars synodic period (2.14 years) with mission configurations that closely match NASA's design reference mission.

Nomenclature

$A_{x,C}$	=	tether cross-sectional area at location x between the center of mass and the countermass, m^2
$A_{x,H}$	=	tether cross-sectional area at location x between the center of mass and the habitat module, m^2
$a_{\max}$	=	maximum acceleration, m/s^2
m_C	=	countermass, kg
m_H	=	habitat module mass, kg
m_P	=	propellant mass, kg
m_T	=	tether mass, kg
V_C	=	countermass velocity relative to the system center of mass, m/s
V_{char}	=	material characteristic velocity, m/s
V_H	=	habitat velocity relative to the system center of mass, m/s
V_∞	=	hyperbolic excess speed, m/s
V^*	=	nondimensional velocity
x	=	distance along the tether from the center of mass, m
ΔV	=	change in velocity, m/s
ρ	=	tether material density, kg/m^3
σ	=	tether material tensile strength, Pa

Introduction

ONE possible configuration of the tether transport facility is depicted in Fig. 1. The transport facility spins, so that the astronauts in the habitat module experience an acceleration similar to the gravitational acceleration they normally experience on Earth. The momentum of the rotating tether system might be used to provide a propellant-free boost for returning the astronauts to Earth after an aborted Mars landing.

Space-based tethered transportation systems can eliminate or reduce the need for expendable propellant.[1−9] Cosmo and Lorenzini[4] present an excellent overview of potential tether applications. For space-based systems, tapered tether designs minimize the mass and the structural loads[1−5,9] Puig-Suari et al.[3] discuss the importance of minimization of the mass for a tether sling transportation system. Jokic and Longuski[9] extend this work by designing tether slings stationed on Phobos for human transportation systems between Earth and Mars.

Possible scenarios for human missions to Mars are widely discussed in the literature.[10−35] The work by Lyne and Townsend[25] details a powered swingby scenario to return astronauts safely to Earth in the event of an aborted Mars landing. Okutsu and Longuski[35] present an investigation of possible free-return trajectories (requiring no propellant expenditure after launch). Their work identifies a potential Earth–Mars–Venus–Earth (E–M–V–E) trajectory with desirable mission parameters in 2014.

In this paper, we develop minimum-mass designs for the tether in a human transport with artificial gravity. We outline a general methodology for the design of a minimum-mass tethered system in a configuration consisting of two end masses connected by a tether, as shown in Fig. 1. We then discuss trajectories with abort capabilities for human missions to Mars. Our analysis identifies some potential trajectories that can use the momentum of the spinning tethered transport to provide the necessary boost to transfer astronauts back to Earth without expending propellant.

Abort Scenarios for Human Missions to Mars

Our investigation aims to identify abort options for human missions to Mars for a worst-case scenario. Ideally, a mission to Mars will be configured to enable the astronauts to return to Earth without requiring an engine to provide a velocity change. Unfortunately, free-return trajectories do not conform to the needs of human missions for all potential launch years. We examine how a spinning tether transportation system might be able to provide the necessary velocity change to return astronauts to Earth. One role of the tethered system is to generate an artificial gravity environment. By spinning the tethered transport, the astronauts in the habitat module experience a centripetal acceleration equal in magnitude to the gravitational acceleration people would normally experience on Earth. Figure 2 shows how a spinning tethered transport system can provide the velocity change required for an Earth–Mars–Earth (E–M–E) abort trajectory. The tether connecting the habitat and countermass modules is severed near apoapsis, so that the habitat has the velocity needed to return the astronauts to Earth. The specific abort scenario depicted in Fig. 2 is one of the solutions we examine in this paper.

We refer to NASA's design reference mission (DRM) to define elements of the tethered transport's mass. Some of the masses

Received 29 October 2003; revision received 25 April 2004; accepted for publication 26 April 2004.

*Ph.D. Candidate, School of Engineering; michaeljokic@telstra.com. Member AIAA.

†Professor, School of Aeronautics and Astronautics, 315 N. Grant Street; longuski@ecn.purdue.edu. Associate Fellow AIAA.

Table 1 System masses for human missions to Mars[24]

System	Mass, kg
Crew-lander-entry mass	60,806
Crew-lander NTR system	26,600
Crew-lander TMI propellant	50,000
Cargo-lander-entry mass	66,043
Cargo-lander NTR system	23,400
Cargo-lander TMI propellant	45,300

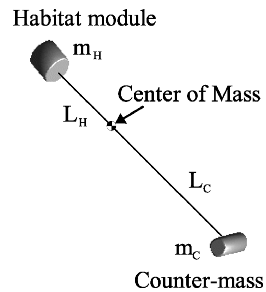

Fig. 1 Possible configuration of space transport with artificial gravity.

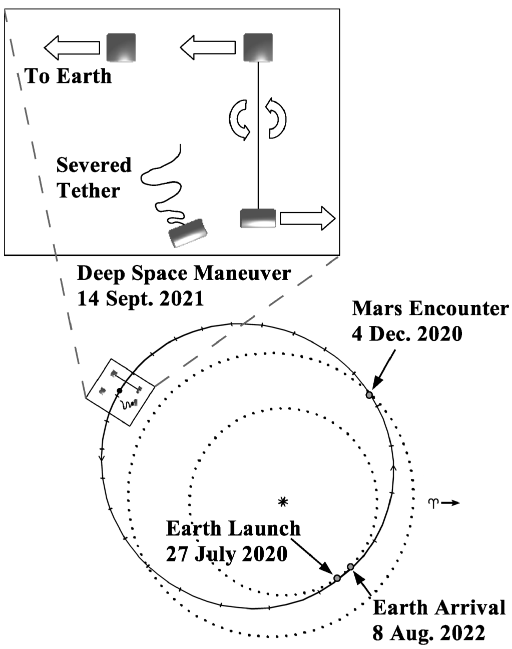

Fig. 2 Aborted mission to Mars with a ΔV achieved by severing the tether.

specified in the DRM are shown in Table 1. In our analysis, the crew-lander-entry mass is the habitat module. We assume that the tethered transport's countermass is the crew-lander, nuclear thermal rocket (NTR) system. One possible alternative tethered transport design might consist of the crew-lander-entry mass tethered to the cargo-lander-entry mass. The emphasis of our examination is on propellant-free abort options that represent worst-case scenarios where the engines on the descent stage fail. If the systems associated with the decent engines do not fail, the masses specified in the DRM suggest that a velocity change of 0.77 km/s is possible. The E–M–E abort trajectory depicted in Fig. 2 requires a 0.5-km/s velocity change near apoapsis to return the habitat module to Earth. Our tether transport design does not require the descent engines to return the habitat module to Earth, but the engines are also capable of producing a 0.5-km/s boost.

Minimum Tether Mass Designs for Artificial Gravity

Design Methodology

Our design methodology for the minimum-mass configuration of the tethered transport begins with a specified value for the speed of the habitat module, relative to the system's center of mass V_H. The characteristic velocity of a tether material is defined as[3]

$$V_{\text{char}} = \sqrt{2\sigma}\big/\rho \tag{1}$$

which represents the maximum tip speed that a uniform (nontapered) tether can support before failure. When the tether is tapered, there is no theoretical maximum tip speed (within practical limits). We define the nondimensional velocity of the habitat module as

$$V_H^* = V_H / V_{\text{char}} \tag{2}$$

The length of the tether from the transport's center of mass to the habitat module is determined by constraint of the acceleration and specification of V_H:

$$L_H = V_H^2 \big/ a_{\max} \tag{3}$$

where $a_{\max}$ is the maximum acceleration experienced by astronauts in the habitat. For the case where the countermass is equal to the habitat mass, the total length of the tether is simply twice the length L_H. In general, however, the end masses are not equal, and the length L_C is dependent on L_H, V_H, and m_C. To determine L_C, we apply the definition of the center of mass for collinear mass elements, with the center of mass defined at the origin

$$m_H L_H + \int_0^{L_H} \rho A_{x,H} x \, \mathrm{d}x - m_C L_C - \int_0^{L_C} \rho A_{x,C} x \, \mathrm{d}x = \sum_{i=1}^{n} x_i m_i = 0 \tag{4}$$

The minimum cross-sectional areas of the tether needed at a distance x from the system center of mass along the lengths L_C and L_H are found from[3]

$$A_{x,C} = A_{L,C} \exp\left[\left(\rho V_C^2 \big/ 2\sigma\right)\left(1 - x^2 L_C^{-2}\right)\right] \tag{5}$$

$$A_{x,H} = A_{L,H} \exp\left[\left(\rho V_H^2 \big/ 2\sigma\right)\left(1 - x^2 L_H^{-2}\right)\right] \tag{6}$$

respectively. The cross-sectional areas at the attachment points of the habitat module and countermass are

$$A_{L,C} = m_C\left(V_C^2 \big/ \sigma L_C\right) \tag{7}$$

$$A_{L,H} = m_H\left(V_H^2 \big/ \sigma L_H\right) \tag{8}$$

Our minimum-mass tether design is tapered from a maximum cross-sectional area at the center of mass to minimum cross-sectional areas at the ends. By evaluation of the integrals and performance of the necessary algebra, Eq. (4) becomes

$$m_H L_H \exp\left(V_H^{*2}\right) = m_C L_C \exp\left(V_H^{*2} L_C^2 \big/ L_H^2\right) \tag{9}$$

Rearranging for L_C produces

$$L_C = m_H L_H / m_C \exp\left\{V_H^{*2} - 1/2 W\left[2 V_H^{*2} m_H^2 \exp\left(V_H^{*2}\right) \big/ m_C^2\right]\right\} \tag{10}$$

where $W(z)$ is the Lambert W function[36] defined as the solution of

$$z = W(z) e^{W(z)} \tag{11}$$

With L_C determined, the velocity of the countermass relative to the transport's center of mass is calculated by

$$V_C = (V_H / L_H) L_C \tag{12}$$

and the nondimensional velocity of the countermass is determined from

$$V_C^* = V_C / V_{\text{char}} \tag{13}$$

The masses associated with the tether lengths L_H and L_C are defined in terms of the nondimensional velocities and the error function as[3]

$$m_{T,H} = m_H\sqrt{\pi}V_H^* \exp\left(V_H^{*2}\right)\mathrm{erf}\left(V_H^*\right) \tag{14}$$

$$m_{T,C} = m_C\sqrt{\pi}V_C^* \exp\left(V_C^{*2}\right)\mathrm{erf}\left(V_C^*\right) \tag{15}$$

respectively. Hence, the total minimum mass of the tether is found by the addition of the mass of the two sections

$$m_T = m_{T,H} + m_{T,C} \tag{16}$$

Substitution of Eq. (10) into Eq. (12) reveals that V_C depends on V_H^*, m_C, and m_H. Therefore, we note from Eqs. (14) and (15) that the tether mass does not depend on the length of the tether, but only on the end masses, tip velocity, and characteristic velocity. Equation (3) indicates that (for a given tip velocity) the length is determined by the maximum acceleration we select for the habitat module.

Mass Performance

We now examine how the countermass-to-habitat-mass ratio and the relative velocity of the habitat V_H affect the mass of the tether. The material selected for the analysis is Zylon, which has a tensile strength of 5.8 GPa and a density of 1560 kg/m^3. Substitution of these properties into Eq. (1) reveals that the characteristic speed of Zylon is 2.7 km/s. One of our metrics for selecting suitable transport designs is the ratio of the tether-mass-to-propellant-mass (m_T/m_P) needed for the deep space maneuver (DSM). We determine the (hypothetical) propellant mass to produce the required change in the habitat module's velocity (DSM) using a single-stage rocket model with an I_{sp} of 379 s.

Figure 3 shows m_T/m_P for a range of habitat throw velocities and ratios of counter-mass-to-habitat-mass (m_C/m_H). The mass of the tether is highly dependent on the desired habitat throw velocity, and so m_T/m_P increases very quickly with increasing throw velocity. As expected, higher values of m_C/m_H for a particular habitat throw velocity produce smaller tether masses and, subsequently, smaller m_T/m_P. Ideally, m_T/m_P should be less than unity, so that the mass of the tether is less than the propellant required to complete a particular abort trajectory. For an m_C/m_H value of 0.5, this condition requires that the habitat throw velocity must be less than about 0.36 km/s. An m_C/m_H of 0.3 requires a change in velocity of less than 0.26 km/s to keep the m_T/m_P ratio less than one. If the mass available for the tether transport is assumed to match the Mars DRM, m_C/m_H is about 0.44. A value of m_T/m_P greater than one is not necessarily a reason to dismiss a design because the system has the added benefit of generating artificial gravity and reducing the entry velocity of the habitat for aerobraking. The habitat module's entry velocity is reduced when the tether is severed, so that the module is released in the opposite direction to the transport's flight path. A lower entry velocity decreases the mass required for heat shielding. In our analysis, we consider designs with m_T/m_P values of up to three as advantageous to human Mars missions.

The ratio of the tether-mass-to-habitat-mass (m_T/m_H) is also investigated as a function of the habitat throw velocity and m_C/m_H. Figure 4 contains curves that show the dependence of m_T/m_H on the required habitat throw velocity. For m_C/m_H values of 0.5 and 0.3, the tether mass remains less than one half of the habitat mass ($m_T/m_H < 0.5$) for habitat throw velocities less than 0.82 and 0.75 km/s, respectively. The performance of the tethered transport, in terms of mass, is highly dependent on the required habitat throw velocity V_H, the strength-to-weight ratio of the tether material, and the ratio of the end masses m_C/m_H.

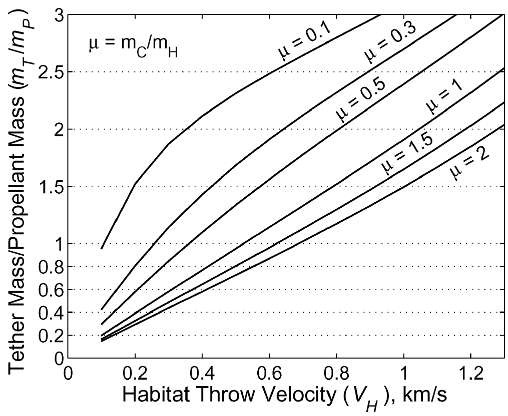

Fig. 3 Tether-mass-to-propellant-mass ratio vs required habitat velocity.

Abort Options via Tethers

We seek trajectories in which a small ΔV can return astronauts to Earth in an acceptable time of flight. If the ΔV is small enough, then our tether design can achieve the maneuver with minimal mass. The spinning tether system has the added benefit of generating an artificial gravity environment. We only allow the ΔV to occur after the tether transport reaches Mars. The restriction of the time of the DSM in this way is consistent with a worst-case scenario in which the decision to abort is made near Mars. For our analysis, we design the tether transport so that the acceleration experienced by the astronauts in the habitat is equal to the acceleration on the surface of the Earth ($1g$).

Table 2 (Refs. 22, 35, and 37) contains some of our constraints for identifying acceptable abort options. We use the conditions to examine E–M–E, E–M–V–E and Earth–Venus–Mars–Earth (E–V–M–E) trajectory paths between 2014 and 2030. The constraints listed are in decreasing order of priority. The V_∞ and the times of flight are presented in the literature as practical design limits for Mars missions. Because the tether serves a dual purpose (of providing artificial gravity and an abort option) we select $m_T/m_P \leq 3$ as a useful design criterion. Short times of flight minimize the exposure of astronauts to high-energy galactic cosmic radiation and solar particle events that can have a significant detrimental effect on the health of the astronauts.[23,25,35]

Table 2 Human mission constraints listed in order of decreasing priority

Mission variable	Constraint
Launch V_∞[a]	$\leq$ 4.5 km/s (Ref. 22)
Mars arrival V_∞	$\leq$ 7.1 km/s (Ref. 37)
Earth arrival V_∞	$\leq$ 9.3 km/s (Ref. 37)
m_T/m_P	≤ 3
TOF, E–M	$\leq$ 180 days (Ref. 35)
Total TOF	$\leq$ 800 days (Ref. 35)

[a]DRM in 2014 requires 3.32 km/s (Ref. 35). Value based on requirement for the 2024 180-day transfer and DRM vehicle masses.

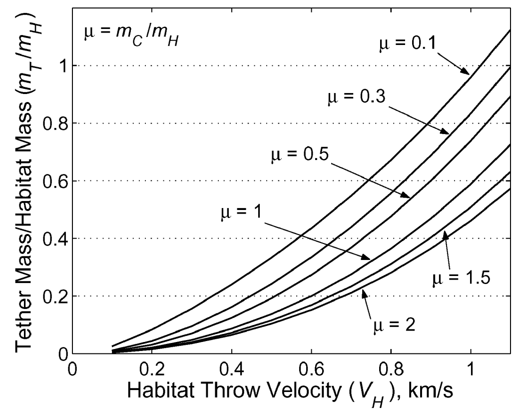

Fig. 4 Tether-mass-to-habitat-mass ratio vs required habitat velocity.

Table 3 E–M–E abort options with a DSM

Launch date, yyyy/mm/dd	Launch V_∞, km/s	Mars arrival V_∞, km/s	Earth arrival V_∞, km/s	DSM, km/s	TOF to DSM, days	TOF to Mars,[a] days	TOF to Earth,[b] days
2014/01/07	3.79	8.30	4.68	1.25	451	158	770
2016/02/27	3.59	8.13	4.77	1.12	496	140	780
2018/05/10[c]	3.90	7.09	5.06	0.71	491	187	759
2020/07/27[c]	4.50	5.59	5.01	0.50	418	134	742
2022/09/12[c]	4.52	4.94	4.90	1.01	443	171	753
2024/10/17[c]	4.56	6.07	4.86	1.12	448	180	753
2026/11/21	4.51	7.83	4.85	0.91	443	172	747
2028/12/23	3.97	8.22	4.69	1.22	433	147	765

[a]TOF to Mars is the TOF for E–M. [b]TOF to Earth is the TOF for E–M–E. [c]Option conforms to all mission constraints.

Table 4 Tether designs for E–M–E abort options

Launch date, yyyy/mm/dd	DSM, km/s	m_C/m_H	Tether mass (m_T), Mg	Tether length ($L_C + L_H$), km	m_T/m_H	m_T/m_P
2014/01/07	1.25	0.44	72.3	417	1.2	3.0
2016/02/27	1.12	0.44	57.8	341	0.95	2.7
2018/05/10[a]	0.71	0.44	24.2	150	0.40	1.9
2020/07/27[a]	0.50	0.44	12.5	77.8	0.21	1.4
2022/09/12[a]	1.01	0.44	47.4	284	0.78	2.5
2024/10/17[a]	1.12	0.44	58.1	343	0.96	2.7
2026/11/21	0.91	0.44	38.8	236	0.64	2.3
2028/12/23	1.22	0.44	69.1	400	1.1	2.9

[a]Option conforms to all mission constraints.

E–M–E Trajectories

Patel et al.[27] examine potential E–M–E free-return trajectories in some detail. Our investigation, however, allows for a small ΔV in the trajectory to ensure that the conditions of Table 2 are met. Table 3 contains the E–M–E options obtained for launch years between 2014 and 2028, where we find the minimum total ΔV from the trajectory optimization program MIDAS.[38] By restricting the mission times of flight, we are able to manipulate the MIDAS output to conform to our constraints (in some cases). There are no free-return solutions for the conditions of Table 2. We note that 2018, 2020, 2022, and 2024 contain launch opportunities that closely match the mission constraints. In all of these cases, the required DSMs can be achieved by severing the tether. Figure 2 shows the 2020 abort scenario. As we noted earlier, the 0.5- and 0.71-km/s DSMs can be achieved when the propellant stored on the transport for descent to the surface of Mars is expended. In all of the cases presented, the time of flight (TOF) to return to Earth is less than the imposed 800-day limit.

Table 4 shows the tether designs needed to achieve the DSMs of the E–M–E abort trajectories. The mass ratio m_T/m_P for the 2018 and 2020 cases are 1.9 and 1.4, respectively. Only the opportunities identified in 2018 and 2020 have a tether mass that is less than half the habitat mass ($m_T/m_H < 0.5$). Our 2018 and 2020 solutions require tether lengths of 150 and 77.8 km. If the maximum acceleration in Eq. (1) is set to equal the acceleration on the surface of Mars ($0.38g$) these lengths increase to 394 and 205 km. The tether lengths in both cases are similar to other tether transfer systems.[3,6,8] For a specified tip velocity, the mass ratios are not affected by a change in the assumed maximum acceleration. We also identified opportunities in 2016, 2026, and 2028, which meet our mass ratio limit for the tether, but the arrival velocities at Mars are larger than the established 7.1-km/s constraint.

E–M–V–E Trajectories

We searched for possible E–M–V–E abort trajectories using STOUR,[39] a patched-conic propagator. Figure 5 presents the trajectories found between 2014 and 2031 with a launch V_∞ equal to 4.5 km/s, a maximum DSM between Mars and Venus of 0.8 km/s, and a minimum flyby altitude of 200 km. We searched for viable trajectories, which require a launch V_∞ between 3.4 and 4.6 km/s, using an increment of 0.1 km/s. The cases with a launch V_∞ of 4.5 km/s are represented in Fig. 5 because this is the upper limit determined for the DRM configuration and to ensure clarity. Despite the large number of solutions available in 2014, an allowance for small ΔV does not result in opportunities in all launch years. Our search does not reveal any potential trajectories in 2022. A large number of trajectories requiring little, or no, ΔV are shown in Fig. 6. All of the trajectories shown in Fig. 6 meet our design requirements, including the V_∞ at Earth and Mars. We selected our final solutions from the STOUR output by displaying the data in graphs such as those in Figs. 5 and 6.

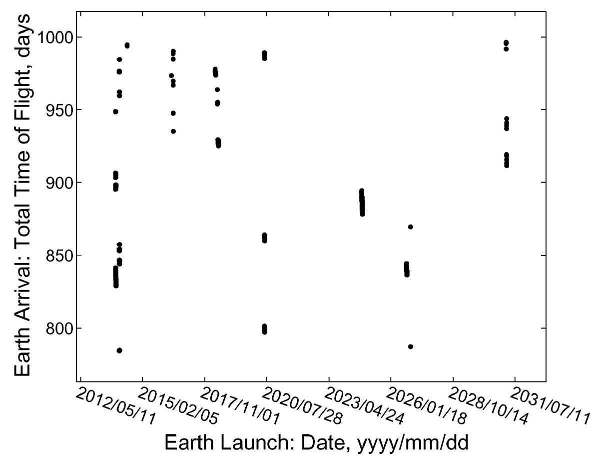

Fig. 5 E–M–V–E trajectories (2014–2031) with maximum TOF ≤ 1000 days.

Table 5 contains our best options for E–M–V–E abort trajectories between 2014 and 2031. We found opportunities in 2014 and 2020, that meet our design constraints. The 2014 abort option is a free-return scenario, which is in agreement with the solution found by Okutsu and Longuski.[35] Whereas the remaining trajectories listed in Table 5 violate the design constraints, the opportunity identified in 2024 only significantly exceeds the limits in the total time of flight (881 days). Table 6 lists the tether transport designs corresponding to the reported E–M–V–E abort trajectories. There are no design requirements based on the 2014 trajectory because it represents a

Table 5 E–M–V–E abort options with a DSM

Launch date, yyyy/mm/dd	Launch V_∞, km/s	Mars arrival V_∞, km/s	Earth arrival V_∞, km/s	DSM, km/s	TOF to Mars,[a] days	TOF to Earth,[b] days
2014/01/13[c]	3.6	6.98	4.81	0.00	170	800
2016/06/14	4.5	6.11	6.84	0.80	370	935
2018/06/13	4.5	4.75	5.04	0.15	262	925
2020/06/24[c]	4.5	4.43	5.86	0.76	168	800
2024/10/16	4.5	5.91	7.52	0.38	184	881
2026/10/07	4.3	4.35	8.63	0.79	263	835
2029/04/23	4.5	8.27	5.52	1.22	388	941
2031/03/01	4.5	7.07	5.32	0.48	380	912

[a]TOF to Mars is the TOF for E–M. [b]TOF to Earth is the TOF for E–M–E. [c]Option conforms to all mission constraints.

Table 6 Tether designs for E–M–V–E abort options

Launch date, yyyy/mm/dd	DSM, km/s	m_C/m_H	Tether mass (m_T), Mg	Tether length ($L_C + L_H$), km	m_T/m_H	m_T/m_P
2014/01/13[a]	0.00	0.44	____[b]	____[b]	____[b]	____[b]
2016/06/14	0.80	0.44	30.3	186	0.50	2.1
2018/06/13	0.15	0.44	1.20	7.47	0.02	0.48
2020/06/24[a]	0.76	0.44	27.5	170	0.45	2.0
2024/10/16	0.38	0.44	7.38	46.1	0.12	1.1
2026/10/07	0.79	0.44	29.6	182	0.49	2.1
2029/04/23	1.22	0.44	69.0	400	1.1	2.9
2031/03/01	0.48	0.44	11.5	72.0	0.19	1.4

[a]Option conforms to all mission constraints.
[b]There are no geometric requirements for the tether when the DSM is zero.

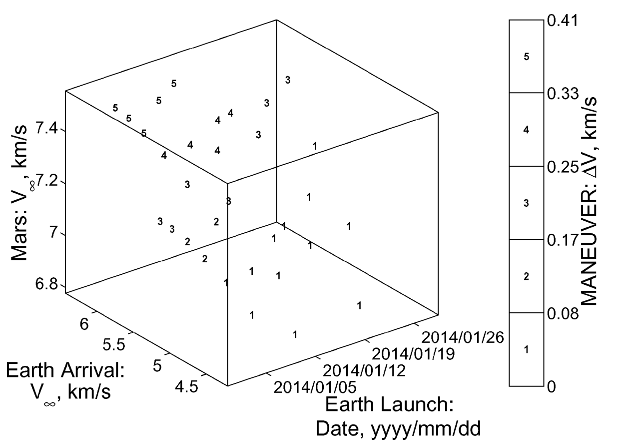

Fig. 6 2014 E–M–V–E trajectory opportunities with TOF < 810 days.

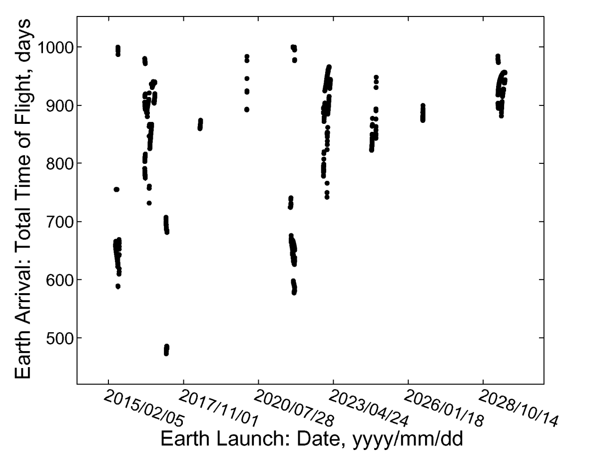

Fig. 7 E–V–M–E trajectories (2014–2031) with maximum TOF ≤ 1000 days.

free-return option. The 2020 trajectory requires a ΔV of 0.76 km/s, which corresponds to a tether with a length of 170 km and a mass ratio m_T/m_P of 2.

E–V–M–E Trajectories

Our search of E–V–M–E trajectories between 2014 and 2031 uncovered numerous launch opportunities. Figure 7 shows potential trajectories with a launch V_∞ equal to 4.5 km/s, a minimum flyby altitude of 200 km, and a maximum DSM between Mars and Earth of 0.9 km/s. As with the E–M–V–E cases, we searched for trajectories with launch V_∞ between 3.4 and 4.6 km/s using an increment of 0.1 km/s. We see in Fig. 7 that trajectories exist with a TOF less than 800 days in 2015, 2016, 2017, 2021, and 2023. A more detailed representation of the 2021 family of trajectories is shown in Fig. 8. A number of trajectories exist in 2021, that require little, or no, ΔV. Unfortunately, the TOF to Mars for these trajectories exceeds the 180-day limit. Because of the flyby of Venus occurring before arrival at Mars, the E–V–M–E trajectory option always has a longer TOF to Mars than the 180-day constraint. Unlike the E–M–V–E trajectory option, the flyby of Venus is a compulsory element of

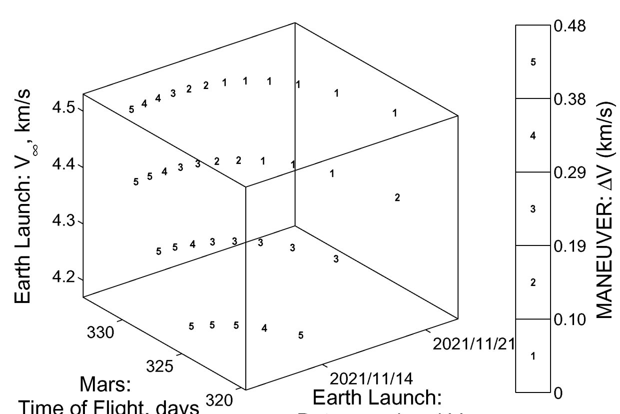

Fig. 8 E–V–M–E trajectory options for 2021 with TOF < 600 days.

Table 7 E–V–M–E abort options with a DSM

Launch date, yyyy/mm/dd	Launch V_∞, km/s	Mars arrival V_∞, km/s	Earth arrival V_∞, km/s	DSM, km/s	TOF to Mars,[a] days	TOF to Earth,[b] days
2015/06/12[c]	4.5	5.20	9.30	0.90	352	588
2016/08/03	4.5	6.23	7.42	0.42	662	757
2017/03/29[c]	4.5	5.33	8.03	0.00	367	681
2018/06/11	4.5	6.08	6.20	1.08	725	973
2020/02/29	4.5	6.66	4.62	0.24	589	961
2021/11/22[c]	4.5	5.42	6.48	0.00	323	582
2023/01/30	4.5	7.17	7.52	0.00	630	766
2024/09/25	3.6	6.99	8.11	0.76	599	930
2026/07/31	4.5	12.5	13.10	0.00	521	886
2028/02/23	4.5	8.62	15.89	1.23	586	770
2029/06/14	4.5	4.70	8.18	0.00	650	868

[a]TOF to Mars is the TOF for E–M. [b]TOF to Earth is the TOF for E–M–E. [c]Option conforms to all mission constraints.

Table 8 Tether designs for E–V–M–E abort options

Launch date, yyyy/mm/dd	DSM, km/s	m_C/m_H	Tether mass (m_T), Mg	Tether length ($L_C + L_H$), km	m_T/m_H	m_T/m_P
2015/06/12[a]	0.90	0.44	38.0	231	0.62	2.3
2016/08/03	0.42	0.44	8.94	55.9	0.15	1.2
2017/03/29[a]	0.00	0.44	—[b]	—[b]	—[b]	—[b]
2018/06/11	1.08	0.44	54.0	320	0.89	2.6
2020/02/29	0.24	0.44	3.15	19.7	0.05	0.76
2021/11/22[a]	0.00	0.44	—[b]	—[b]	—[b]	—[b]
2023/01/30	0.00	0.44	—[b]	—[b]	—[b]	—[b]
2024/09/25	0.76	0.44	27.8	171	0.46	2.0
2026/07/31	0.00	0.44	—[b]	—[b]	—[b]	—[b]
2028/02/23	1.23	0.44	70.4	407	1.2	2.9
2029/06/14	0.00	0.44	—[b]	—[b]	—[b]	—[b]

[a]Option conforms to all mission constraints. [b]There are no geometric requirements for the tether when the DSM is zero.

Table 9 Selected abort options (with a DSM) for human missions to Mars

Launch date, yyyy/mm/dd	Path	Launch V_∞, km/s	Mars arrival V_∞, km/s	Earth arrival V_∞, km/s	DSM, km/s	m_T/m_P	TOF to Mars, days	TOF to Earth, days
2014/01/13[a]	E–M–V–E	3.60	6.98	4.81	0.00	—[b]	170	800
2015/06/12	E–V–M–E	4.50	5.20	9.30	0.90	2.3	352	588
2016/02/28[a]	E–M–E	3.59	8.13	4.77	1.12	2.9	140	780
2018/05/10[a]	E–M–E	3.90	7.09	5.06	0.71	1.9	187	759
2020/07/27[a]	E–M–E	4.50	5.59	5.01	0.50	1.4	134	742
2021/11/22	E–V–M–E	4.50	5.42	6.48	0.00	—[b]	323	582
2022/09/12[a]	E–M–E	4.52	4.94	4.90	1.01	2.5	171	753
2024/10/17[a]	E–M–E	4.56	6.07	4.86	1.12	2.7	180	753
2026/11/21[a]	E–M–E	4.51	7.83	4.85	0.91	2.3	172	747
2028/12/28[a]	E–M–E	3.97	8.22	4.69	1.22	2.9	147	765

[a]Option conforms to all mission constraints. [b]There are no geometric requirements for the tether when the DSM is zero.

the mission to Mars in the E–V–M–E path.The crew's exposure to potential radiation hazards during the transfer to Mars is increased by adopting the E–V–M–E trajectory.

The best options for the E–V–M–E abort trajectories are listed in Table 7. Many of the options are free returns that do not require a ΔV. Note that only 2018 and 2028 require a ΔV greater than 1 km/s. From the trajectories listed in Table 7, we identify the 2015, 2017, and 2021 opportunities as potential abort options. Although the TOFs to Mars are all over 300 days, the total TOF to arrive at Earth for these trajectories are all less than 700 days. The 2021 opportunity is the best E–V–M–E alternative with a TOF to Mars of 323 days and a TOF to return to Earth of only 582 days. Table 8 presents the tether designs needed for the E–V–M–E abort trajectories. There are no geometric constraints for the tether transport facility in the five free-return options. We note that in all of the cases presented, $m_T/m_P < 3$.

Discussion

Table 9 contains our best abort scenario trajectory options between 2014 and 2030. Opportunities that closely match our mission constraints exist in every Earth–Mars synodic period (approximately 2.14 years). Although the 2016, 2026, and 2028 options have Mars arrival $V_\infty > 7.1$ km/s, we have accepted the opportunities because their relatively high DSMs are useful: the spinning tether can reduce the magnitude of the arrival V_∞ at Mars so that the entry conditions achieve the mission constraints. The E–M–E trajectories recommended for 2018 and 2020 require DSMs of 0.71 and 0.5 km/s, which can be achieved by using the descent engines. Although the DSMs of the remaining E–M–E options are too large for the descent engines alone, the DSMs might be realized via a combination of the tether rotation and descent engines. The final preferred case in 2014 is a free-return trajectory and, therefore, the tethered transport's geometry is independent of the trajectory.

We note that most of the trajectory options listed in Table 9 follow the E–M–E path. The only E–M–V–E case listed occurs in 2014, and E–V–M–E cases are suggested for 2015 and 2021. As noted earlier, the E–V–M–E trajectory options violate the TOF design limits and increase the radiation risk for astronauts. We present free-return trajectory options for 2014 and 2021. The most difficult years for abort scenarios that meet our design constraints appear to be 2016, 2026, and 2028. A logical approach to reduce the mass of the tether for our preferred trajectory options is to combine the spinning tether system with the descent stage engines. Of course, this would prevent the abort scenarios from being propellant free.

Conclusions

A minimum-mass, spinning tether transport can facilitate the propellant-free return of astronauts to Earth in the event of an aborted landing on Mars. We have identified abort scenarios in every Earth–Mars synodic period between 2014 and 2030 that closely match the mission parameters of NASA's DRM. Most of our recommended abort options follow an Earth–Mars–Earth path with a small DSM. Our minimum-mass tether design methodology enabled us to develop transport configurations for the abort scenarios with a tether-mass-to-propellant-mass ratio of less than 3. Relaxation of the constraints for human missions to Mars and improvements in tether strength-to-weight ratios may produce more abort options. Further investigation of potential transport configurations is needed to determine practical design limits for the tether mass ratios. The abort scenarios and artificial-gravity tether transports presented in this paper have the potential to play an important role in missions to Mars.

Acknowledgments

The first author was supported in this work by an Australian Postgraduate Award and a departmental scholarship administered by the University of Queensland. We thank Masataka Okutsu (Purdue Ph.D. Candidate) for his assistance.

References

[1]Moravec, H., "A Non-Synchronous Orbital Skyhook," *Journal of the Astronautical Sciences*, Vol. 25, No. 4, 1977, pp. 307–327.

[2]Tillotson, B., "Tether as Upper Stage for Launch to Orbit," AIAA Paper 89-1585, May 1989.

[3]Puig-Suari, J., Longuski, J. M., and Tragesser, S. G., "A Tether Sling for Lunar and Interplanetary Exploration," *Acta Astronautica*, Vol. 36, No. 6, 1995, pp. 291–295.

[4]Cosmo, M. L., and Lorenzini, E. C. (ed.), *Tethers in Space Handbook*, 3rd ed., Smithsonian Astrophysical Observatory, Cambridge, MA, 1997.

[5]Kuchnicki, S. N., Tragesser, S. G., and Longuski, J. M., "Dynamics of a Tether Sling," American Astronautical Society, AAS Paper 97-605, Aug. 1997.

[6]Bogar, T. J., Bangham, M. E., Forward, R. L., and Lewis, M.J., "Hypersonic Airplane Space Tether Orbital Launch (HASTOL) System: Interim Study Results," AIAA Paper 99-4802, Nov. 1999.

[7]Hoyt, R. P., and Uphoff, C. W., "Cislunar Tether Transport System," *Journal of Spacecraft and Rockets*, Vol. 37, No. 2, 2000, pp. 177–186.

[8]Nordley, G., and Forward, R., "Mars–Earth Rapid Interplanetary Tether Transport System: 1. Initial Feasibility Analysis," *Journal of Propulsion and Power*, Vol. 17, No. 3, 2001, pp. 499–507.

[9]Jokic, M. D., and Longuski, J. M., "Design of a Tether Sling for Human Transportation Systems Between Earth and Mars," *Journal of Spacecraft and Rockets*, Vol. 41, No. 6, 2004, pp. 1010–1015.

[10]Hollister, W. M., "Mars Round Trip Trajectories," AIAA Paper 64-67, Aug. 1964.

[11]Sohn, R. L., "Manned Mars Trips Using Venus Flyby Modes," *Journal of Spacecraft and Rockets*, Vol. 3, No. 2, 1966, pp. 161–169.

[12]Aldrin, B., "Cyclic Trajectory Concepts," SAIC Science Applications International Corporation, Interplanetary Rapid Transit Study Meeting, Oct. 1985.

[13]Friedlander, A. L., Niehoff, J. C., Byrnes, D. V., and Longuski, J. M., "Circulating Transportation Orbits Between Earth and Mars," AIAA Paper 86-2009, Aug. 1986.

[14]Hoffman, S. J., Friedlander, A. L., and Nock, K. T., "Transportation Node Performance Comparison for a Sustained Manned Mars Base," AIAA Paper 86-2016, Aug. 1986.

[15]Nock, K. T., and Friedlander, A. L., "Elements of a Mars Transportation System," *Acta Astronautica*, Vol. 15, No. 6/7, 1987, pp. 505–522.

[16]Wilson, S., "Fast Round Trip Mars Trajectories," AIAA Paper 90-2934, Aug. 1990.

[17]Williams, S. N., and Longuski, J. M., "Low Energy Trajectories to Mars via Gravity Assist from Venus to Earth," *Journal of Spacecraft and Rockets*, Vol. 28, No. 4, 1991, pp. 486–488.

[18]Wolf, A. A., "Free Return Trajectories for Mars Missions," American Astronautical Society, AAS Paper 91-123, Feb. 1991.

[19]Byrnes, D. V., Longuski, J. M., and Aldrin, B., "Cycler Orbit Between Earth and Mars," *Journal of Spacecraft and Rockets*, Vol. 30, No. 3, 1993, pp. 334–336.

[20]Lyne, J. E., and Braun, R. D., "Flexible Strategies for Manned Mars Missions Using Aerobraking and Nuclear Thermal Propulsion," *Journal of the Astronautical Sciences*, Vol. 41, No. 3, 1993, pp. 339–347.

[21]Walberg, G. D., "How Shall We Go to Mars? A Review of Mission Scenarios," *Journal of Spacecraft and Rockets*, Vol. 30, No. 2, 1993, pp. 129–139.

[22]Hoffman, S. J., and Kaplan, D. I., "Human Exploration of Mars: The Reference Mission of the NASA Mars Exploration Study Team," NASA SP 6107, March 1997.

[23]Zubrin, R., *The Case for Mars*, 1st ed., Simon and Schuster, New York, 1997, pp. 75–101,113–132.

[24]Drake, B. G., "Reference Mission Version 3.0 Addendum to the Human Exploration of Mars: The Reference Mission of the NASA Mars Exploration Study Team," NASA Rept. EX-98-036, June 1998.

[25]Lyne, J. E., and Townsend, L. W., "Critical Need for a Swingby Return Option for Early Manned Mars Missions," *Journal of Spacecraft and Rockets*, Vol. 35, No. 6, 1998, pp. 855–856.

[26]Lyne, J. E., Wercinski, P., Walberg, G., and Jits, R., "Mars Aerocapture Studies for the Design Reference Mission," American Astronautical Society, AAS Paper 98-110, Feb. 1998.

[27]Patel, M. R., Longuski, J. M., and Sims, J. A., "Mars Free Return Trajectories," *Journal of Spacecraft and Rockets*, Vol. 35, No. 3, 1998, pp. 350–354.

[28]Munk, M. M., "Departure Energies, Trip Times and Entry Speeds for Human Mars Missions," American Astronautical Society, AAS Paper 99-103, Feb. 1999.

[29]Bishop, R. H., Byrnes, D. V., Newman, D. J., Carr, C. E., and Aldrin, B., "Earth–Mars Transportation Opportunities: Promising Options for Interplanetary Transportation," American Astronautical Society, AAS Paper 00-255, March 2000.

[30]Nock, K. T., "Cyclical Visits to Mars via Astronaut Hotels," Phase I Final Rept. NASA Inst. for Advanced Concepts, Univ. Space Research Association Research Grant 07600-049, Nov. 2000.

[31]Aldrin, B., Byrnes, D., Jones, R., and Davis, H., "Evolutionary Space Transportation Plan for Mars Cycling Concepts," AIAA Paper 2001-4677, Aug. 2001.

[32]Chen, J. K., McConaghy, T. T., Okutsu, M., and Longuski, J. M., "A Low-Thrust Version of the Aldrin Cycler," AIAA Paper 2002-4420, Aug. 2002.

[33]Chen, K. J., Landau, D. F., McConaghy, T. T., Okutsu, M., Longuski, J. M., and Aldrin, B., "Trajectory Analysis and Design of Mars Cyclers: Preliminary Assessment," AIAA Paper 2002-4422, Aug. 2002.

[34]McConaghy, T. T., Longuski, J. M., and Byrnes, D. V., "Analysis of a Class of Earth–Mars Cycler Trajectories," *Journal of Spacecraft and Rockets*, Vol. 41, No. 4, 2004, pp. 622–628.

[35]Okutsu, M., and Longuski, J. M., "Mars Free Returns via Gravity Assist from Venus," *Journal of Spacecraft and Rockets*, Vol. 39, No. 1, 2002, pp. 31–36.

[36]Corless, R. M., Gonnet, G. H., Hare, D. E. G., Jeffrey, D. J., and Knuth, D. E., "On the Lambert W Function," *Advances in Computational Mathematics*, Vol. 5, No. 4, 1996, pp. 329–359.

[37]George, L. E., and Kos, L. D., "Interplanetary Mission Design Handbook: Earth-to-Mars Mission Opportunities and Mars-to-Earth Return Opportunities 2009-2024," NASA TM-1998-208533, July 1998.

[38]Sauer, C. G., Jr., "MIDAS: Mission Design and Analysis Software for the Optimization of Ballistic Interplanetary Trajectories," *Journal of the Astronautical Sciences*, Vol. 37, No. 3, 1989, pp. 768–775.

[39]Rinderle, E. A., "Galileo User's Guide, Mission Design System, Satellite Tour Analysis and Design Subsystem," Jet Propulsion Lab., JPL Publication D-263, California Inst. of Technology, Pasadena, CA, July 1986.

C. Kluever
Associate Editor